processes

MDPI

Article

Mechanisms of Permeability Alteration via Gel Based on Nuclear Magnetic Resonance

Bin Zou [1,2,4], Chuanzhi Cui [1,2,*], Wangang Zheng [4,5], Weiyao Zhu [3], Haishun Feng [4,5], Wei Chu [4,5], Tiantian Yu [1,2,5] and Zhongping Zhang [4,5]

[1] State Key Laboratory of Deep Oil and Gas, China University of Petroleum (East China), Qingdao 266580, China
[2] School of Petroleum Engineering, China University of Petroleum (East China), Qingdao 266580, China
[3] School of Resources and Safety Engineering, University of Science and Technology Beijing, Beijing 100083, China
[4] Shengli Oilfield Company, SINOPEC, Dongying 257000, China; chuwei.slyt@sinopec.com
[5] Shandong Provincial Key Laboratory of Heavy Oil Production Technology, Dongying 257000, China
* Correspondence: ccz1231128@163.com; Tel.: +86-15776554018

Abstract: DPR refers to the fact that the reduction in the permeability of the water phase is much greater than the reduction in the permeability of the oil phase when a water-based gel seals porous media. In order to clarify the mechanisms of the gel-plugging pore pathway and the principle of the oil phase and water-phase permeability change, gel-plugging core replacement experiments and NMR T2 scanning experiments were conducted in this work. Based on the nuclear NMR T2 spectroscopy, the core blocked with Cr (III)–acetate–HPAM gel is divided into five stages (a plug injection and seal gel-formation stage, an oil-phase repulsion stage, a stopping-gel reabsorption stage, an oil-phase reinjection stage, and a subsequent water-drive stage) for displacement and scanning, and the signal changes of various phases in the displacement process are studied. The principle of an oil-phase permeability increase after Cr (III)–acetate–HPAM gel plugging, and the principle of a disproportionate decrease in water-phase permeability in the subsequent water-flooding stage were finally revealed. According to the results, the difference in the permeability leads to some diversity in NMR T2 curves, but the final conclusions for the mechanisms are consistent. They show a significant decrease in core permeability of 3.5×10^{-3} μm^2 and 0.8×10^{-3} μm^2 after gel plugging. With the injection of the oil phase, the permeability of the oil phase keeps increasing from 0.13×10^{-3} μm^2 to 0.76×10^{-3} μm^2 in the core permeability of 3.5×10^{-3} μm^2. Similarly, the permeability of the oil phase increases from 0.03×10^{-3} μm^2 to 0.19×10^{-3} μm^2 in the core permeability of 0.8×10^{-3} μm^2. During the oil-phase replacement phase, gel replacement in the large pores is the main cause of the increase in oil-phase permeability, and as the replacement process progresses, the mechanism for the increase in oil-phase permeability changes, and gel dehydration becomes the main mechanism for the increase in oil-phase permeability.

Keywords: polymer gel; plugging; phase permeability; NMR T2 scanning experiments

check for updates

Academic Editor: Qingbang Meng

Received: 5 December 2024
Revised: 13 January 2025
Accepted: 6 February 2025
Published: 11 February 2025

Citation: Zou, B.; Cui, C.; Zheng, W.; Zhu, W.; Feng, H.; Chu, W.; Yu, T.; Zhang, Z. Mechanisms of Permeability Alteration via Gel Based on Nuclear Magnetic Resonance. *Processes* **2025**, *13*, 497. https://doi.org/10.3390/pr13020497

Copyright: © 2025 by the authors. Licensee MDPI, Basel, Switzerland. This article is an open access article distributed under the terms and conditions of the Creative Commons Attribution (CC BY) license (https://creativecommons.org/licenses/by/4.0/).

1. Introduction

After a long period of exploitation in the oilfield, there are a large number of dominant pathways in the deep part of the reservoir, severe non-homogeneity in primary and post-primary pathways, a large difference in fluid mobility, a rapid rise in the water cut of the oil well, and the crude oil can be driven out smoothly in the higher permeability formations, but

it is hard to recover in the lower permeability formations [1,2]. Continued water injection will only pass through the rock formations of high permeability and then be recovered, resulting in severe inefficient circulation and affecting recovery rates. Deep profile control techniques are one of the most effective ways to improve the swept volume of the injected fluid and control ineffective circulation [3–7]. Polymer gel, with the characteristics of easy injection, high stability, and strength, is the most widely used profile control plugging agent, with gel treatments accounting for 60% of the EOR program in the US [8–11]. After gel is injected into the fracture, disproportionate filtration from the fracture wall occurs, and a portion of the polymer and chromium ions will filtrate loss from the fracture wall into the matrix, affecting the gel-forming strength and the plugging effect [12,13]. Li et al. [14] prepared a new type of gel by coating polyethyleneimine into multiple W/O/W emulsions. Core experiments showed that the new gel system exhibited good plugging performance in fractured low-permeability reservoirs. Li et al. [15] used a weak gel profile control agent through core experiments and found that it achieves good injection performance, transport properties, and characteristics of plugging. Xie et al. [16] investigated the main mechanism of the plugging phenomenon and analyzed the theoretical grouping design experiments of the oil–water pathway diversion, gel dehydration, and adsorption hysteresis. The results showed that the adsorption hysteresis of the gel on the rock wall is the main mechanism causing the plugging phenomenon and decreasing the water-phase permeability more than the oil-phase permeability. The commercial application of nuclear magnetic resonance (NMR) scanning technology also provides a new method for research [7,17–20]. In NMR T2 testing, if a sample is placed in a static magnetic field, tiny bar magnets will all face in the same direction. The resultant magnetic moment of each hydrogen nucleus is represented as a macroscopic magnetization vector. The magnitude of the magnetization vector is proportional to the number of hydrogen nuclei, which is proportional to the volume of the fluid. In NMR T2 spectroscopy, the signal amplitude represents the macroscopic magnetization vector. Therefore, the larger the signal amplitude, the larger the free fluid volume. Since both oil and water contain hydrogen nuclei, it is difficult to separate them using magnetic signals [21]. However, if the cores are immersed in $MnCl_2$ solution for a long enough time, the paramagnetic ions Mn^{2+} will diffuse into the water, so the relaxation time of water will decrease at the instrument detection limit. In addition, Mn^{2+} is insoluble in oil, so the relaxation time of oil will remain unchanged, and the NMR T2 test can be used as an indicator of changes in oil saturation [22]. Wu [23] designed core experiments and NMR T2 scanning experiments under different polymer concentrations. The results showed that a high-concentration polymer solution achieves a better plugging effect than a low-concentration polymer solution, and the high-concentration polymer solution effectively reduces the pore space and has a good sealing effect on the large pore pathway.

In addition, for selective water plugging agents, including Cr (III)–acetate–HPAM gel, some researchers [24–26] also found that the gel reduces the permeability of the water phase more than the oil phase in the porous media, which is called a disproportionate permeability reduction (DPR). In order to explain the DPR phenomenon, some work has been carried out. Dawe and Zhang [27] found that oil and water pass through the gel via different mechanisms. When oil passes through the gel, it carries some of the water in the gel to widen the pathway; however, when water passes through, it causes the gel to absorb water and swell. Grattoni et al. [28] suggested that the permeability of the gel to water increases with an increasing flow rate and that this dependent behavior is due to its elasticity; as for the polymer concentration, the effect varies and decreases with its increase. Ganguly et al. [29] found that there was a functional relationship between oil–water permeability and the imposed pressure gradient, the DPR value decreased with the increase in the pressure gradient, and the influence of the pressure gradient on oil-phase

permeability is due to the deformation of the pore structure caused by the pressure gradient. Nguyen et al. [30] found that, with the increase in the pressure gradient after dehydration, the DPR value of strong gel decreased, but the DPR value of weak gel increased. Al-Shajalee et al. [31] found that the adsorption of polymers on the pore wall can reduce the roughness of the pore surface, thereby promoting the flow of the non-wetting phase. The entanglement of polymers reduces the channels available for water flow and is considered one of the reasons for the reduction in water permeability. Seright et al. [32] found that dewatering caused an increase in oil-phase permeability using X-rays. Liang et al. [33] used NMR T2 technology to analyze different core samples treated with polymer gels. They found that gel hydration blocking the flow channels was the main mechanism for the increase in oil-phase permeability. However, the mechanism of DPR is not yet clear, and further research is necessary in view of its importance.

In this paper, the experiments were divided into two main parts, one for the Cr (III)–acetate–HPAM gel-blocking core replacement experiments and the other for the NMR T2 scanning experiments. In the core replacement experiments, cores with different permeabilities were selected to simulate different levels of formation conditions and to compare the permeability changes of the oil phase and the water phase. The NMR T2 scanning experiments were used to study the changes in the signal amplitude under the different oil and water injection volumes and to analyze the mechanism of the oil-phase permeability rise and the principle of a disproportionate reduction in water-phase permeability in the subsequent water-flooding stage. The objective of this study is to clarify the mechanism of gel-blocking pore channels and the principle of oil-phase and water-phase permeability changes, to analyze the changes in the oil and water phases during the gel displacement process, including the plug injection and seal gel-formation stage, the oil-phase repulsion stage, the stopping-gel reabsorption stage, the oil-phase reinjection stage, and the subsequent water-drive stage, and to reveal the control mechanism of DPR at different stages.

2. Experiments

2.1. Experimental Materials

Polyacrylamides are peculiar in reducing the permeability of water more than oil [34]. As chromium III is added to form a crosslinked polymer, the permeability further decreases compared to the un-crosslinked polymer [35]. In the experiments, the gel formula is as follows: 0.3% hydrolyzed polyacrylamide (HPAM), 0.4 % chromium III (Cr^{3+}), and 0.3% NaCl. Among these, HPAM has a molecular weight of 12 million, with 25% hydrolysis and 98% purity. The core permeability used in the experiments is 3.5×10^{-3} μm^2 and 0.8×10^{-3} μm^2 to simulate different levels of permeability. The core diameter is 2.51 cm, and the length is 7.1 cm. Before the start of the experiments, the core is evacuated via a vacuum pump to make it 100% saturated with water. All NMR T2 data in this section are inverted via noise reduction using the T2 spectral inversion program written by David Medellin, postdoctoral fellow at the University of Texas at Austin [36].

Figure 1 shows that the experiments are divided into two parts. The first part is the core displacement experiments, and the second part is the NMR T2 scanning experiments. In the core replacement experiments, the ISCO pump provides a constant pressure gradient or injection rate, controlled via a six-way valve; the oil or water phase is injected into the core. The confining pressure pump provides the confining pressure for the core holder. As the NMR T2 scanner currently does not support online repetition scanning, after each injection of a fixed multiple of pore volumes of oil or water, displacement is stopped, the core is removed and scanned with the NMR T2 scanner then reinserted into the core holder, and confining pressure is added for displacement. The NMR T2 experiments mainly include three parts: the magnet probe, the control box, and the data display.

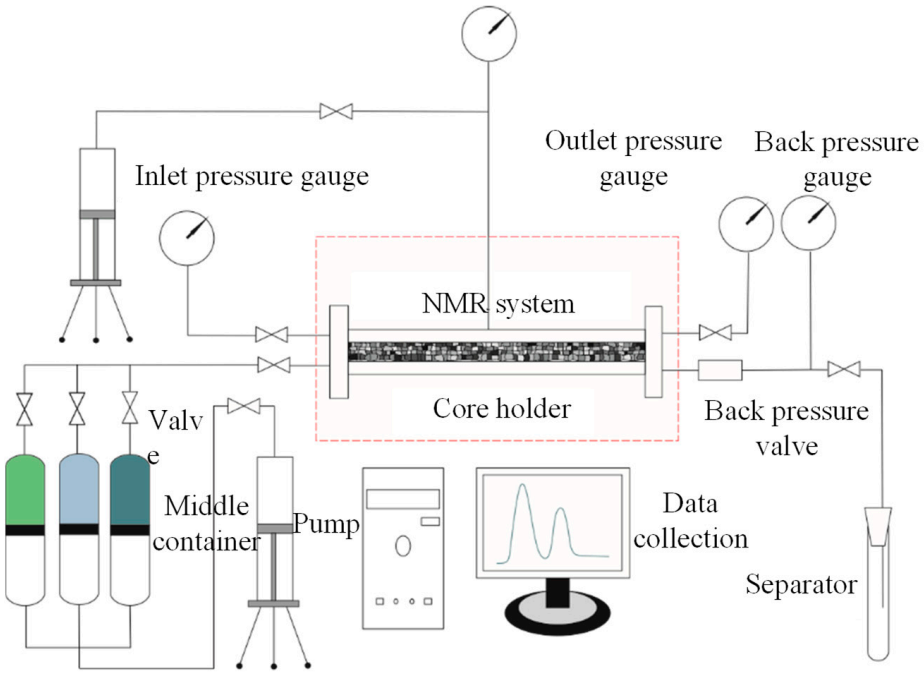


Figure 1. Experimental flow diagram.

2.2. Experimental Procedure

The experiments were divided into five stages. In the first stage, the Cr (III)–acetate–HPAM crosslinked polymer with 6 times the pore volume was injected into the core and then sealed and put into an incubator at 50 °C to form gel for 24 h. In the second stage, the oil phase was injected into the core at a constant rate, and the displacement was stopped for every 10 pore volumes (PVs) of the oil phase injected; the core was removed for NMR T2 scanning and the displacement resumed. In the third stage, the injection of the oil phase was stopped when it reached a certain amount, and then NMR T2 scanning was conducted at different times. In the fourth stage, the oil-phase injection was resumed, the change in injection pressure was observed, and NMR T2 scanning was performed at the same time. In the fifth stage, the water phase was injected into the core at a constant rate, and NMR T2 scanning was taken after every 20 PV water phase had been injected; then, oil-phase injection was resumed. In order to reduce the influence of external factors on the T2 spectra results, three sets of experiments were conducted for each type of experiment in this paper. The average and variance of the results were calculated and plotted. To better distinguish the hydrogen nuclei in the oil and water phases, we incorporated the paramagnetic substance Cr (III) into the gel solution to reduce the relaxation time of the water phase based on the study used by Clerke et al. [22]. As a result, the NMR T2 data can reveal the pattern of changes in oil-phase saturation.

3. Results and Discussion

3.1. The Principle of DPR

Figure 2 shows the change in permeability during the sequential displacement of the oil (blue line) and the water (red line) after the gel plugging. It indicates that the permeability of the core decreased substantially [37,38], falling from 3.5×10^{-3} μm^2 to 0.13×10^{-3} μm^2. With the oil-phase injection, the permeability of the oil phase kept increasing from 0.13×10^{-3} μm^2 to 0.76×10^{-3} μm^2.

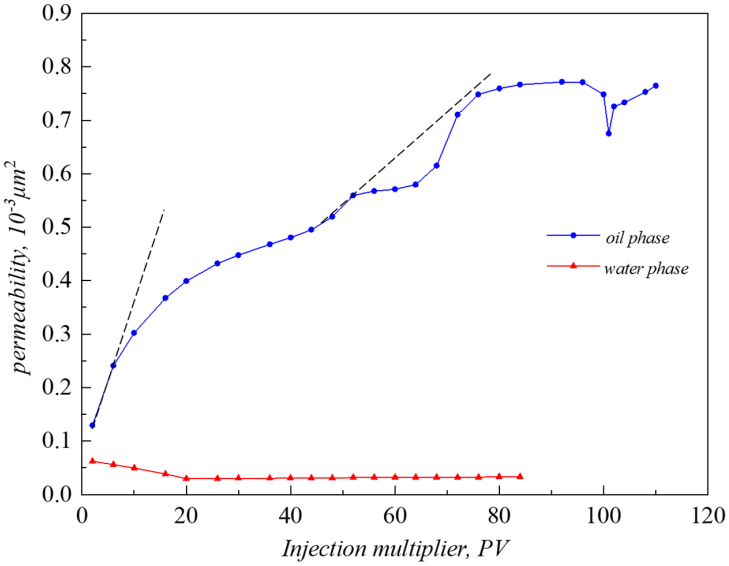


Figure 2. Change in permeability of oil and water phases (3.5×10^{-3} μm^2).

Firstly, the rate of increase in oil-phase permeability showed a gradual decrease, and the two gradient dashed lines can be seen to reveal an obvious decrease when the injection volume was 7 PV, indicating that the oil-phase percolation pathway was affected. There are two main reasons for the oil-phase percolation pathway; one is a gel displacement mechanism, and the other is a gel dehydration mechanism. If the increase in the oil-phase permeability is caused by a mechanism, the oil-phase permeability gradient should remain unchanged, which is inconsistent with the law in Figure 2. In the process of displacement, it was found that only in the initial stage of the oil-phase displacement was a part of the gel discharged, and almost no gel was produced later. Therefore, it can be inferred that the mechanism of the oil-phase permeability increase had changed. In the initial stage, gel production was the main mechanism. With the displacement process, the gel dehydration mechanism played a dominant role.

When the oil injection volume reached 50 PV, we stopped the injection and stewed for 12 h before the next displacement. When the injection volume reached 65 PV, the permeability of the oil phase was shown with blue dots, but the actual permeability was less than this value. The dehydrated gel absorbs water and swells when in contact with free water. This causes the gel to absorb water and swell, which results in a narrowing of the percolation pathways and an increase in the flow resistance [39].

Since the conditions for the gel to absorb water, again, involve the dehydration of the gel and the presence of free water, the injection of the oil phase was stopped when it reached 100 PV, and the NMR T2 scanning was then performed several times over a period of 40 h. When the oil-phase injection was resumed (101 PV), a relatively significant reduction in permeability was observed, demonstrating that some free water remained in the pores at this time and also indicating the existence of gel reabsorption. With the continuous injection of the oil phase, the permeability of the oil phase rapidly increased again, indicating that the reabsorption of water from the gel could only restore the plugging capacity to a limited extent, and the plugging capacity of the gel after water absorption was lower than that of the gel before dehydration.

Figure 3 shows the permeability change of oil–water sequential displacement after a 0.8×10^{-3} μm^2 case was plugged by the gel. Similar to the 3.5×10^{-3} μm^2 case, it can be seen that the permeability of the oil phase gradually increased from 0.03×10^{-3} μm^2 to 0.19×10^{-3} μm^2. The permeability gradient of the oil phase changed significantly at around 10 PV, indicating that the main mechanism had changed from gel displacement to

gel dehydration. When the injection amount reached 50 PV, the injection was stopped for 14 h, and the oil-phase permeability was also significantly reduced, indicating that the gel also swelled. After the injection of the 100 PV oil phase, water flooding was initiated, and the core permeability was rapidly reduced to very low values and remained at very low levels [37].

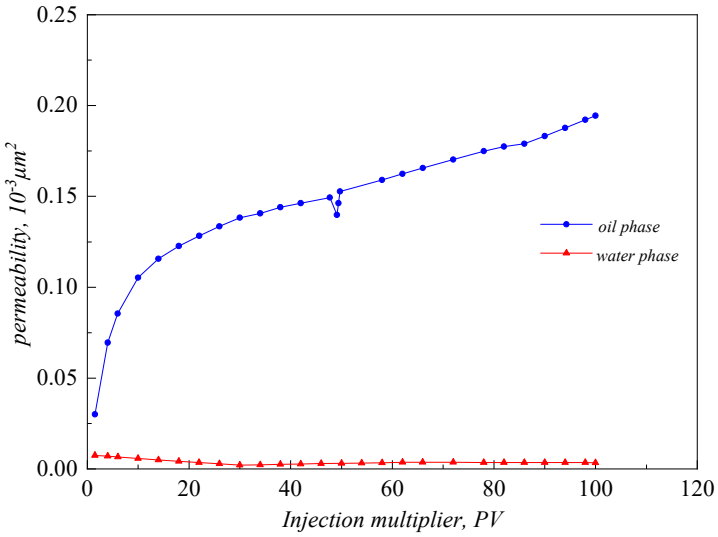


Figure 3. Change in permeability of oil and water phases (0.8×10^{-3} μm^2).

3.2. Variation in the Ratio of Oil-Phase to Water-Phase Permeability

Figure 4 shows the ratio of oil-phase to water-phase permeability (R_{ow}) during the experiment. It can be seen that the overall trend of R_{ow} is constantly increasing, which fully reflects the DPR behavior of the gel profile control. For the core with a permeability of 3.5×10^{-3} μm^2, Row increases slowly, with a maximum increase of 23.1. For the core with a permeability of 0.8×10^{-3} μm^2, Row increases rapidly in the early stage of displacement, with a maximum increase of 64.0, and then slowly decreases, indicating that the main mechanism has changed from gel displacement to gel dehydration. Under the same injection PV-number conditions, the R_{ow} of the core with a permeability of 0.8×10^{-3} μm^2 is 2.1 times greater than that of the core with a permeability of 3.5×10^{-3} μm^2. This result shows that gel profile control is a promising technology for improving recovery in the development of low-permeability reservoirs.

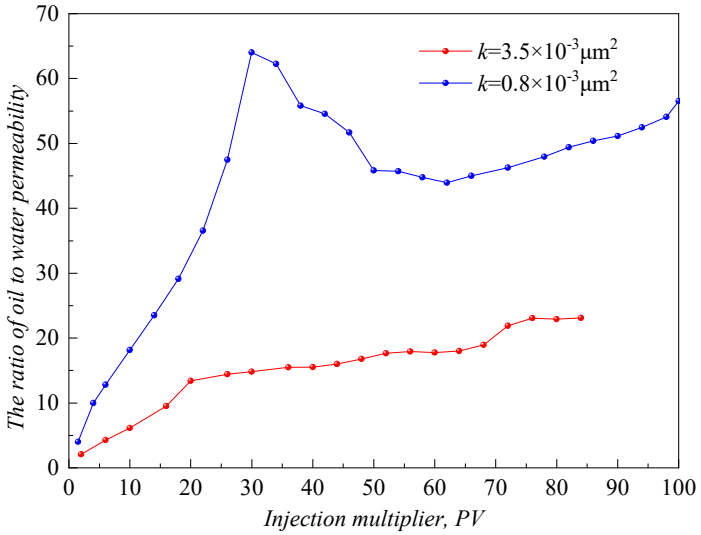


Figure 4. Changes in the ratio of oil–water permeability during gel flooding.

4. Discussion

4.1. Mechanism of Increased Oil-Phase Permeability

Through the change in permeability during the displacement of the above two permeability cores, it can be seen that the Cr (III)–acetate–HPAM gel has obvious selective water-plugging properties. Using NMR T2 techniques, we further investigated the reasons for the disproportionate permeability changes in the oil and water phases.

Figure 5 shows that there is a clear double peak in the image of saturated water. Since the magnitude of the relaxation time can approximately characterize the size of the pores, and after saturating a fluid, the signal amplitude represents the share of the pores corresponding to the different relaxation times, a high proportion of small pores are present in this core. After the saturated gel, the signal amplitude of the large pores decreases significantly, the signal of the small and medium pores (40 to 200 ms) increases significantly, and the signal in the small pores decreases weakly.

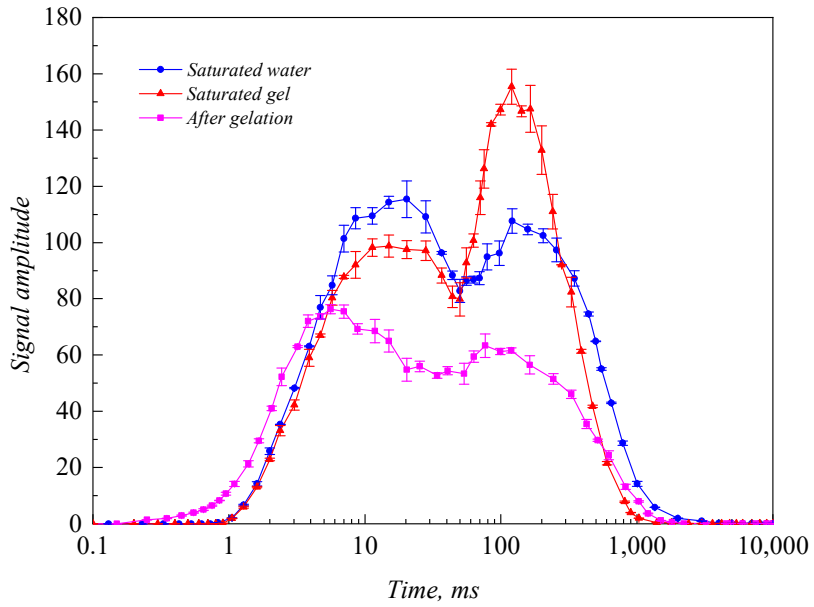


Figure 5. T2 spectra of different injected fluids at the initial stage.

Since the components change, the signal amplitude cannot be understood simply as a change in the pore share. The reduction in signal amplitude is essentially due to the addition of the paramagnetic substance Cr (III) to the solution, which is able to cut the relaxation time of the signal. For signals in large pores, the relaxation time is reduced because of the paramagnetic substance, thus reducing the signal amplitude in large pores, and the reduced amount of signal is added to the medium pores in the range of 40 to 200 ms, so that the signal amplitude in large pores is reduced externally, and the signal amplitude in medium pores is increased. The larger the pore space, the more pronounced the effect of the paramagnetic substance. The T2 spectrum after gelation is represented by the pink curve, which shows a further decrease in the signal amplitude in both the large and small pores compared to the state of the gel solution when it is first injected. After gelation, the polymer chains form a stable mesh-like 3D envelope structure in the presence of a crosslinked agent, in which the water molecules are bound, leading to a further reduction in signal amplitude. It can be concluded that the signal amplitude of the same volume of free water is significantly higher than that of the gel from the set of curves.

Figure 6 shows the core T2 spectrum data for different oil-phase injection amounts of 3.5×10^{-3} μm^2 case. The details can be seen in Table 1. When the oil reaches 7 PV, the signal amplitude in the large pores is significantly reduced, which means that the amount

of fluid is reduced; this indicates that the core gel is replaced with fluorine oil without a signal in the process. At the same time, this inference can be confirmed by the continuous production of gel at the export end. At this stage, gel removal is the main mechanism of increased oil-phase permeability.

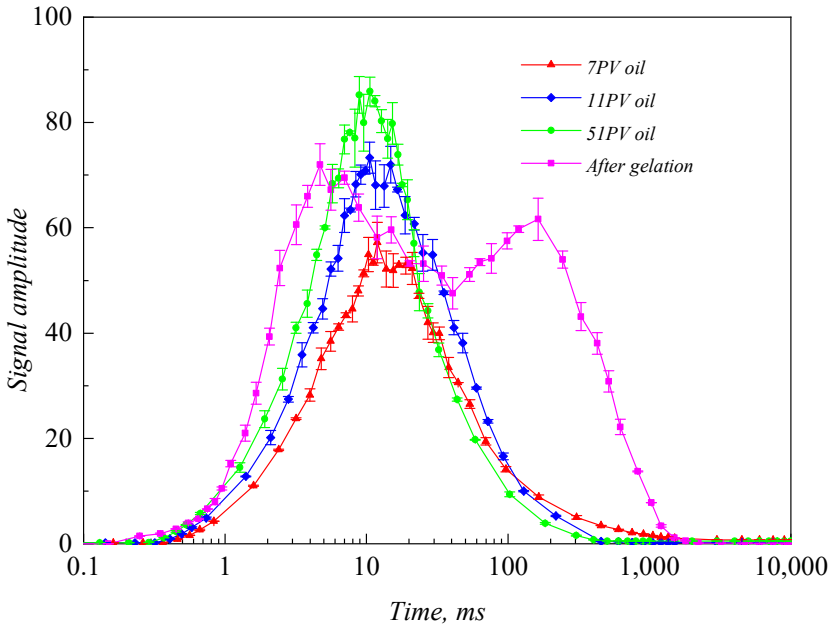


Figure 6. T2 spectra of different oil phase injections (3.5×10^{-3} μm^2).

Table 1. T2 spectra data of different oil phase injections (3.5×10^{-3} μm^2).

Group	Peak 1			Peak 2		
	Start Time	Peak Value	End Time	Start Time	Peak Value	End Time
7 PV oil	0.36	54.92	1906.9	/	/	/
11 PV oil	0.41	73.31	504.17		/	/
51 PV oil	0.26	85.59	504.17	/	/	/
After gelation	0.16	72.00	40.64	40.64	61.64	1506.27

It can be seen that the signal amplitude in the large pores slows down significantly after 7 PV, and there is almost no gel production at the outlet, so the gel is no longer the main reason for the continued formation of the oil-phase flow pathway. As the signal amplitude is proportional to the fluid volume, the increase in the signal amplitude should be due to an increase in gel or free water. As all the pores are saturated prior to the replacement, no more gel would have been squeezed into these pores, and the amount of gel in the pores would not have increased. Therefore, the increase in signal in the small pores is due to the increase in the free water. The water in the gel will be released from the gel due to the oil-phase pressure difference.

Part of the free water is bound in the small pores, and as the signal amplitude of the free water is significantly higher than that of the gel, this results in a rise in the signal amplitude in the small pore space. During this process, the signal amplitude in the larger pores also shows a slow decrease. It can be inferred that the gel in the large pore space is also dehydrated, but the free water from the gel is hardly retained in the large pore space, and even if some of it is retained, the amount of retention is not sufficient to compensate for the reduction in signal, so the signal amplitude in the large pore space shows a slow decrease [17].

Figure 7 shows the core T2 spectrum data for different oil-phase injection amounts of 0.8 × 10^{-3} μm^2 case, which is significantly different from the 3.5 × 10^{-3} μm^2 case. The details can be seen in Table 2. The signal amplitude of the small pore space on the left side of this core is negligible compared to the signal of the large pore space, which indicates that the proportion of small pore space in this core is extremely small compared to the large pore space, and its variation is difficult to have a pattern, so it is not very meaningful to study it; accordingly, we mainly discuss the signal variation in the large pore space on the right side. During the first 10 PV of oil-phase injection, the signal amplitude in the large pore space decreases rapidly, especially in the first 2 PV. At this stage, the permeability of the oil phase gradually increases, accompanied by the output of gel at the outlet end, indicating that the production of gel is the main reason for the increase in oil-phase permeability in this stage. As the oil-phase replacement continues, the signal amplitude in the large pores continues to decrease, and the change in the small pores is negligible. The gradient in oil-phase permeability shows a more pronounced decrease in the gradient of increase in oil-phase permeability at approximately 10 PV. As for the signal amplitude, the peak signal drops from 170 to 110 for the first 10 PV at a rate of 6/PV.

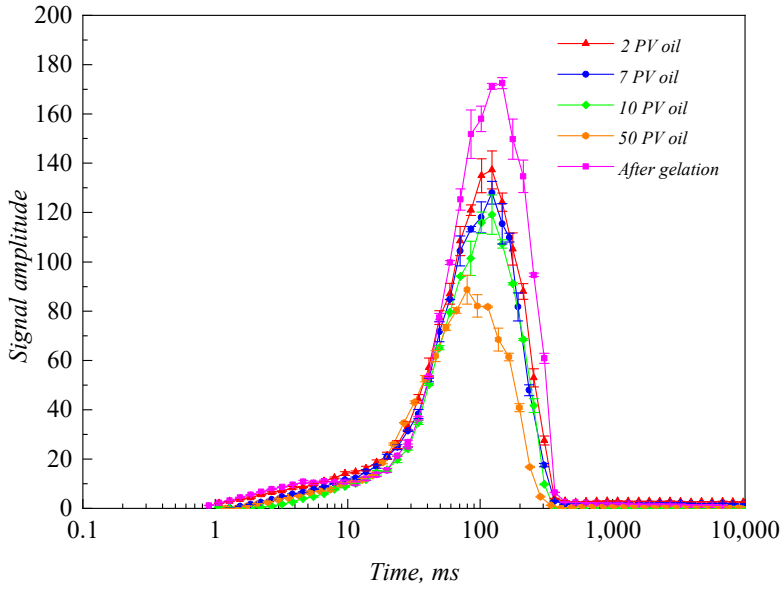


Figure 7. T2 spectrum of different oil phases' injections (0.8 × 10^{-3} μm^2).

Table 2. T2 spectra data of different oil phase injections (0.8 × 10^{-3} μm^2).

Group	Peak		
	Start Time	Peak Value	End Time
2 PV oil	1.07	137.28	426.02
7 PV oil	1.28	127.99	404.17
10 PV oil	1.36	119.16	385.41
50 PV oil	1.49	88.70	365.08
After gelation	0.89	172.48	438.25

However, the signal amplitude from 10 PV to 50 PV decreases from 55 to 42, with a decrease rate of 0.33/PV. The change in the NMR T2 signal also shows that the mechanism of oil-phase permeability increase has changed with the displacement, from gel displacement to gel dehydration. It is difficult to observe the continuous production of gel at the core outlet around 10 PV. With the continuous oil displacement, the dehydration of gel still mainly occurs in the middle pores, and the peak value of the T2 spectrum can be observed

to exhibit a left shift. Due to the continuous erosion of fluorine oil without a signal, most of the free water of the gel out is produced, so overall, the signal amplitude in the large pores shows a downward trend, although part of the free water will stay in the pore space, but still not enough to make up for the amount of signal reduction, so the overall signal amplitude still decreases.

Based on the above analysis, it can be concluded that the main mechanism of the initial increase in the matrix after gel plugging is that the gel is driven away, leading to the formation of the oil-phase flow pathway. With the further progress of oil-phase displacement, the main mechanism changes, and the dehydration and contraction of the gel under the action of oil-phase pressure difference become the main reasons for the rising oil-phase permeability. Although the T2 spectrum data of two cores with different permeability exhibit diversity, the overall pattern is consistent. Similar results can be seen in Liang et al.' s work; they obtained that different correlation between a core's pore size and the relaxation time [33]. There exist two peaks in the 2.3-Darcy case, and the left peak disappears in the 0.8-Darcy case. As the relaxation time crudely represents the size of a pore, it can be considered that the 2.3-Darcy case's maximum pore is larger than the other.

The following will analyze the change pattern of the fluid signal in the pore space with the subsequent oil-phase displacement. Figure 8 shows the variation curve of the T2 spectrum of a core with a permeability of 3.5×10^{-3} μm^2 as the oil phase is continuously injected. It can be seen that the signal amplitude in the large pore space remains almost constant from 51 PV to 100 PV as the oil-phase replacement process proceeds. Combined with Figure 6, the signal amplitude in the large pore space before 51 PV remains slowly decreasing, which shows that, as the dehydration process continues, the gel concentration in the large pores gradually increased, dehydration becomes more and more difficult and almost stagnated at the later stage. On the contrary, the signal amplitude in the small pores continues to rise, as the gel dewatering process continues, the oil-phase flow pathways become wider, the oil phase has a higher degree of contact with the gel, and the gel in the small pores continues to dewater, resulting in the free water volume in the small pores continuing to increase, so the signal amplitude remains rising, and the oil-phase permeability is rising.

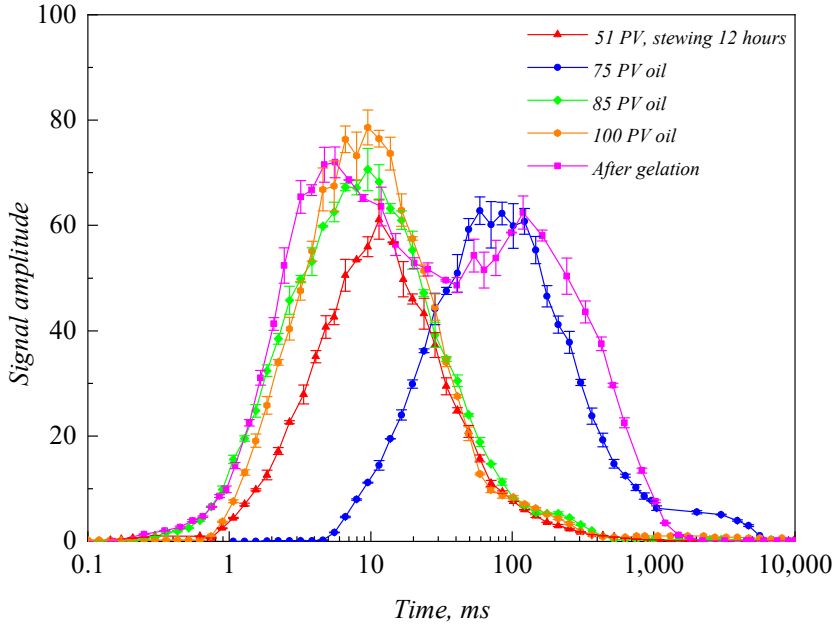


Figure 8. T2 spectrum of different oil phases' injections (3.5×10^{-3} μm^2).

4.2. Mechanism of Decreased Water-Phase Permeability

Figure 9 shows the core T2 spectrum data for the oil and water phases' permeability changes of 3.5×10^{-3} μm^2 case. Compared with the T2 spectral curve with an oil-phase injection volume of 110 PV, a significant rise in signal amplitude is observed in all pores. The signal amplitude in the large pores returns to a state close to that just after gelation. The increase in signal amplitude in the large pores is mainly due to the reabsorption of water into the gel after dehydration and the occupation of some of the pore pathways previously occupied by signal-free fluorine oil by free water. According to the previous analysis, during the initial injection stage of the oil phase, part of the gel in the large pores will be driven away, and part will be dehydrated so that the dehydrated gel will absorb water and push some of the fluorine oil out of the pore space, which will lead to an increase in signal amplitude. In addition, some of the free water will replace some of the non-signal fluorine oil, which will also lead to an increase in signal amplitude. The gel, after absorbing water, will swell and block the existing flow pathway, so some water needs to pass through the gel. Because of the extremely low water permeability in the gel, the gel's water absorption in the large pores is a reason for the DPR.

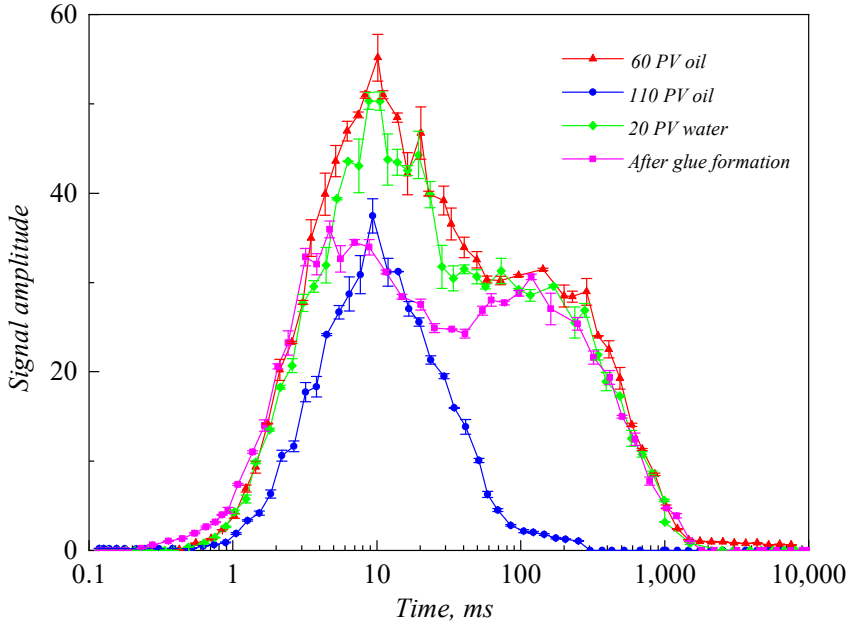


Figure 9. T2 spectrum of different oil and water phases' injections (3.5×10^{-3} μm^2).

From the previous analysis, it is known that part of the gel in the large pores is replaced with the oil phase, and this part of the space is currently occupied by free water and residual oil. Figure 9 shows that the signal of water will be much larger than that of gel for the same amount of gel and water. The details can be seen in Table 3. Based on the fact that the amplitude of the core signal after water flooding is similar to that after gelling, it can be inferred that there is a large amount of residual oil without signal in the hole. Therefore, it can be inferred that the residual oil is a cause of the DPR. With the subsequent water flooding, the signal in the large pores remains constant, the signal in the small pores also stabilizes, and the permeability of the water phase remains almost constant.

Figure 10 shows the core T2 spectrum data for the oil and water phases' permeability changes of 0.8×10^{-3} μm^2 case. The details can be seen in Table 4. Compared with the T2 spectral curve at 100 PV, the amplitude of the signal in the large pores gradually increases during the water flooding in the first 60 PV. The increase in signal amplitude only occurs in the large pores because of the existence of the gel. At the same time, it can be seen that, unlike the core with permeability of 3.5×10^{-3} μm^2, the signal amplitude in the large pores

with a permeability core of 0.8 × 10^{-3} μm^2 does not return to the signal state after just gelling but is far less than the signal peak after just gelling. Since the large pores of this core are much narrower than the 3.5 × 10^{-3} μm^2 core, the reabsorption of the gel will further squeeze the flow pathway, and a lot of residual oil still remains in the pores, and the flow pathway is much less able to bind free water. Thus, the water absorption of the gel, as well as the retention of partial free water, causes only a limited rise in the signal amplitude. Because its signal amplitude is significantly lower than that after gelation, and the signal of the water phase is significantly higher than that of the gel, it can be inferred that a large amount of residual oil is trapped in the pores.

Table 3. T2 spectra data of different oil and water phase injections (3.5 × 10^{-3} μm^2).

Group	Peak 1			Peak 2		
	Start Time	Peak Value	End Time	Start Time	Peak Value	End Time
60 PV oil	0.42	55.16	58.41	58.41	31.36	1762.09
110 PV oil	0.55	37.46	304.13	/	/	/
20 PV water	0.42	50.34	56.99	56.99	29.49	1762.53
After gelation	0.18	35.96	41.04	41.04	61.64	1806.83

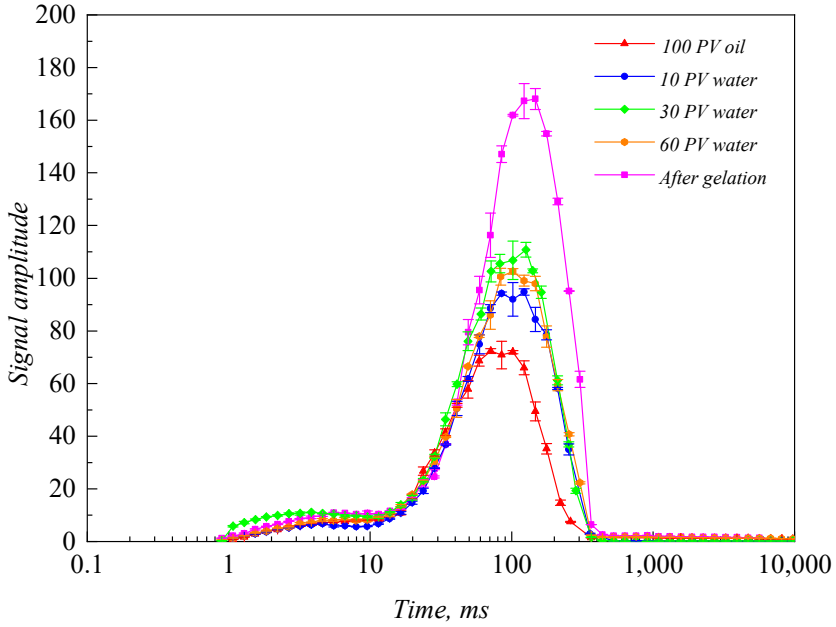


Figure 10. T2 spectrum of different oil and water phases' injections (0.8 × 10^{-3} μm^2).

Table 4. T2 spectra data of different oil and water phase injections (0.8× 10^{-3} μm^2).

Group	Peak		
	Start Time	Peak Value	End Time
100 PV oil	0.88	72.34	365.33
10 PV water	0.88	94.79	367.17
30 PV water	0.88	110.84	370.41
60 PV water	0.88	102.63	371.08
After gelation	0.89	168.06	374.25

Therefore, the water absorption expansion of the gel and the high residual oil saturation are the important reasons for blocking the flow pathway. This result can be verified from Deng et al.' s research; it also shows that the plugging mechanism of gel for small

and large pores in core is obviously different [17]. A considerable amount of water needs to flow through the gel or through the gel membrane, but the permeability of the water phase decreases rapidly due to the extremely low permeability of the water phase in the gel. Figure 9 shows that the permeability of the core decreases rapidly from 0.19×10^{-3} μm^2 to about 0.01×10^{-3} μm^2, and the permeability is maintained at a constant level as the water flooding continues. The swelling of the gel, the hindering effect of the residual oil, and the flow of the water phase in the gel are the causes of the DPR. This is consistent with the studies of other scholars [33,40], which showed that the main mechanism leading to DPR is the hydration and swelling of the gel polymer.

5. Conclusions

In this paper, NMR T2 was used to investigate the main mechanisms through which the permeability of Cr (III)–acetate–HPAM gel-treated cores was elevated during oil-phase replacement and unevenly reduced during water-phase replacement. During the oil-phase replacement phase, gel replacement in the large pores is the main cause of the increase in oil-phase permeability, and as the replacement process progresses, the mechanism for the increase in oil-phase permeability changes, and gel dehydration becomes the main mechanism for the increase in oil-phase permeability. For high-permeability matrices, gel dehydration occurs mainly in small and medium pores, while for lower-permeability matrices, gel dehydration occurs mainly in large and medium pores. In the subsequent water flooding, the gel immediately absorbs water and swells, and the permeability of the water phase immediately decreases to very low values. The reasons for the DPR are as follows: (1) The gel absorbs water and swells, and it squeezes the oil-phase flow pathways. (2) A large amount of residual oil is trapped in the flow pathways, severely impeding the flow of the water phase. (3) Water has a low flow capacity in the gel. Due to the swelling of the gel and the obstruction of the residual oil, most of the water can only flow through the gel itself. For highly permeable matrices, gel absorption occurs in all the pores, whereas for lower-permeability matrices, it occurs mainly in the large and medium pores. The overall trend of R_{ow} is increasing, which fully reflects the DPR behavior of gel-profile control. Under the same injection PV-number conditions, the R_{ow} of the core with the permeability of 0.8×10^{-3} μm^2 is 2.1 times that of the core with the permeability of 3.5×10^{-3} μm^2, and this result shows that gel-profile control is a technology with the potential to improve recovery in the development of low-permeability reservoirs.

Forthcoming research endeavors will be devoted to studying the mobile fluids in low-permeability tight/shale oil reservoirs by utilizing NMR T2, providing a theoretical basis for the further exploration and development of oil reservoirs.

Author Contributions: This paper is a collaborative work of all the authors. B.Z. and C.C. proposed the idea and wrote the manuscript. B.Z. and W.Z. (Weiyao Zhu) designed the experiment. C.C. and W.Z. (Wangang Zheng) performed the experiment. Z.Z. and H.F. analyzed the experimental data. W.C. and T.Y. revised and edited the paper. All authors have read and agreed to the published version of the manuscript.

Funding: This work was supported by the National Key R&D Program of China (Grant Number 2018YFA0702400).

Data Availability Statement: The figures used to support the findings of this study are included in the article.

Conflicts of Interest: Authors Bin Zou, Wangang Zheng, Haishun Feng, Wei Chu and Zhongping Zhang were employed by Shengli Oilfield Company, SINOPEC. The remaining authors declare that the research was conducted in the absence of any commercial or financial relationships that could be construed as a potential conflict of interest.

References

1. Ju, Y.; Gong, W.; Chang, W.; Sun, M. Effects of pore characteristics on water-oil two-phase displacement in non-homogeneous pore structures: A pore-scale lattice Boltzmann model considering various fluid density ratios. *Int. J. Eng. Sci.* **2020**, *154*, 103343. [CrossRef]
2. Lu, G.; Zhang, L.; Liu, Q.; Xu, Q.; Zhao, Y.; Li, X.; Deng, G.; Wang, Y. Experiment analysis of remaining oil distribution and potential tapping for fractured-vuggy reservoir. *J. Pet. Sci. Eng.* **2022**, *208*, 109544. [CrossRef]
3. Wang, L.L.; Wang, T.F.; Wang, J.X.; Tian, H.T.; Chen, Y.; Song, W. Enhanced oil recovery mechanism and technical boundary of gel foam profile control system for heterogeneous reservoirs in Changqing. *Gels* **2022**, *8*, 371. [CrossRef] [PubMed]
4. Liu, J.; Almakimi, A.; Wei, M.; Bai, B.; Hussein, I.A. A comprehensive review of experimental evaluation methods and results of polymer micro/nanogels for enhanced oil recovery and reduced water production. *Fuel* **2022**, *324*, 124664. [CrossRef]
5. Temizel, C.; Putra, D.; Zhang, M.; Moreno, R. Smart nanoparticles for conformance improvement in waterflooding. In Proceedings of the SPE/IATMI Asia Pacific Oil & Gas Conference and Exhibition, Jakarta, Indonesia, 17–19 October 2017.
6. Gao, G.; Ji, K.; Zhang, Y.; Liu, X.; Dai, X.; Zhi, B.; Cao, Y.; Liu, D.; Wu, M.; Li, G.; et al. Microbial enhanced oil recovery through deep profile control using a conditional bacterial cellulose-producing strain derived from *Enterobacter* sp. FY-07. *Microb. Cell Factories* **2020**, *19*, 59. [CrossRef] [PubMed]
7. Tang, M.; Wang, C.; Yang, H.; Lu, J.; Yu, H. Experimental investigation on plugging performance of nanospheres in low-permeability reservoir with bottom water. *Adv. Geo-Energy Res.* **2022**, *6*, 95–103. [CrossRef]
8. Leng, G.; Yan, W.; Li, F.; Wang, B.; Yuan, G.; Chu, C.; Li, Y.; Gao, C. Improved oil recovery in sandstone reservoirs with deep profile control technology: A comparative study between modified starch gel and polymer gel. *Geoenergy Sci. Eng.* **2023**, *226*, 211697. [CrossRef]
9. Lashari, Z.A.; Yang, H.; Zhu, Z.; Tang, X.; Cao, C.; Iqbal, M.W.; Kang, W. Experimental research of high strength thermally stable organic composite polymer gel. *J. Mol. Liq.* **2018**, *263*, 118–124. [CrossRef]
10. Han, X.; Zhong, L.; Liu, Y.; Wang, Q.; Wang, C. Experimental study of polyacrylamide polymer gel for profile controlling in high-temperature offshore reservoirs. *Energy Sources Part A Recovery Util. Environ. Eff.* **2024**, *46*, 11133–11147. [CrossRef]
11. Soka, S.; Sidiq, H. Sensitivity analysis of parameters affecting nano-polymer solution for water shutoff in carbonate rocks. *Adv. Geo-Energy Res.* **2022**, *6*, 230. [CrossRef]
12. Wu, Q.; Ge, J.; Ding, L.; Guo, H.; Wang, W.; Fan, J. Insights into the key aspects influencing the rheological properties of polymer gel for water shutoff in fractured reservoirs. *Colloids Surf. A Physicochem. Eng. Asp.* **2022**, *634*, 127963. [CrossRef]
13. Xie, K.; Mei, J.; Cao, W.; Cao, B.; Yao, L.; Zhang, B.; Wang, H.; Guo, K.; Wu, Z.; Yan, K.; et al. Improving oil mechanism of polymer gel fracturing fluid based on filtration displacement. *J. Pet. Sci. Eng.* **2022**, *218*, 111030. [CrossRef]
14. Li, X.; Pu, C.; Wei, H.; Huang, F.; Bai, Y.; Zhang, C. Enhanced oil recovery in fractured low-permeability reservoirs by a novel gel system prepared by sustained-release crosslinker and water-soluble thixotropic polymer. *Geoenergy Sci. Eng.* **2023**, *222*, 211424. [CrossRef]
15. Li, H.; Wang, K.; Han, X.; Zheng, J. Research on heterogeneous compound flooding system based on dispersed particle gel. *Adv. Geo-Energy Res.* **2019**, *3*, 156–164. [CrossRef]
16. Xie, S.; Ye, Z.; Chen, H.; Han, L. The mechanism study of disproportionate permeability reduction by water-soluble polymer gel. *Pet. Geol. Recovery Effic.* **2010**, *17*, 52–54+58+114. (In Chinese)
17. Deng, Z.; Liu, M.; Qin, J.; Sun, H.; Zhang, H.; Zhi, K.; Zhu, D. Mechanism study of water control and oil recovery improvement by polymer gels based on nuclear magnetic resonance. *J. Pet. Sci. Eng.* **2022**, *209*, 109881. [CrossRef]
18. Bai, L.; Shi, C.; Tang, K.; Xie, H.; Yang, S.; Zhu, D. Study on migration and plugging performance of polymer gel in fractured cores using nuclear magnetic resonance technology. *Geoenergy Sci. Eng.* **2023**, *227*, 211891. [CrossRef]
19. Saikia, T.; Mejia, L.; Sultan, A.; Balhoff, M.; Hamad, J.A. Visualizing conformance control mechanisms in high-temperature reservoirs: A microfluidic analysis of Pickering emulsified gel systems. *Microfluid. Nanofluid.* **2024**, *28*, 75. [CrossRef]
20. Elsayed, M.; Isah, A.; Hiba, M.; Hassan, A.; Al-Garadi, K.; Mahmoud, M.; El-Husseiny, A.; Radwan, A.E. A review on the applications of nuclear magnetic resonance (NMR) in the oil and gas industry: Laboratory and field-scale measurements. *J. Pet. Explor. Prod. Technol.* **2022**, *12*, 2747–2784. [CrossRef]
21. Liang, B.; Jiang, H.; Li, J.; Gong, C.; Jiang, R.; Qu, S.; Pei, Y.; Yang, H. Investigation of oil saturation development behind spontaneous imbibition front using nuclear magnetic resonance T2. *Energy Fuels* **2017**, *31*, 473–481. [CrossRef]
22. Clerke, E.E.; Coates, G.R.; Hartman, D.E.; Horkowitz, J.P.; Vinegar, H.J. Residual oil saturation measurements in carbonates with pulsed NMR logs. *Log Anal.* **1997**, *38*, SPWLA-1997-v38n2a2.
23. Wu, P. Study on the mechanism and distribution of polymer gel profile control in medium and high permeability reservoirs. *Contemp. Chem. Ind.* **2023**, *52*, 183–186. (In Chinese)
24. Tileuberdi, N.; Nassibullin, B.; Kuli, Z.; Gussenov, I.; Kenzhekhanov, S.; Yin, X.; Sailaukhanuly, Y. Challenges of Gel Treatment Application for Conformance Control. *Eng. Sci.* **2024**, *31*, 1238. [CrossRef]

25. Zhao, Y.; Bai, B. Experimental study of transport behavior of swellable microgel particles in superpermeable channels for conformance control. *SPE J.* **2022**, *27*, 790–805. [CrossRef]
26. Jia, H.; Li, P.; Zhang, Y. Polymer Gel for Water Shutoff in Complex Oil and Gas Reservoirs: Mechanisms, Simulation, and Decision-Making. *SPE J.* **2024**, *29*, 243–259. [CrossRef]
27. Dawe, R.A.; Zhang, Y. Mechanistic study of the selective action of oil and water penetrating into a gel emplaced in a porous medium. *J. Pet. Sci. Eng.* **1994**, *12*, 113–125. [CrossRef]
28. Grattoni, C.A.; Al-Sharji, H.H.; Yang, C.; Muggeridge, A.H.; Zimmerman, R.W. Rheology and permeability of crosslinked polyacrylamide gel. *J. Colloid Interface Sci.* **2001**, *240*, 601–607. [CrossRef]
29. Ganguly, S.; Willhite, G.P.; Green, D.W.; McCool, C.S. Effect of flow rate on disproportionate permeability reduction. In Proceedings of the SPE International Conference on Oilfield Chemistry, Houston, TX, USA, 5–7 February 2003; p. SPE-80205.
30. Nguyen, T.Q.; Green, D.W.; Willhite, G.P.; McCool, C.S. Effects of gelant composition and pressure gradients of water and oil on disproportionate permeability reduction of sandpacks treated with polyacrylamide-chromium acetate gels. *SPE J.* **2006**, *11*, 145–157. [CrossRef]
31. Al-shajalee, F.; Wood, C.; Xie, Q.; Saeedi, A. Effective mechanisms to relate initial rock permeability to outcome of relative permeability modification. *Energies* **2019**, *12*, 4688. [CrossRef]
32. Seright, R.S.; Prodanovic, M.; Lindquist, W.B. X-ray computed microtomography studies of fluid partitioning in drainage and imbibition before and after gel placement: Disproportionate permeability reduction. *SPE J.* **2006**, *11*, 159–170. [CrossRef]
33. Liang, B.; Jiang, H.; Li, J.; Chen, F.; Miao, W.; Yang, H.; Qiao, Y.; Chen, W. Mechanism study of disproportionate permeability reduction using nuclear magnetic resonance T2. *Energy Fuels* **2018**, *32*, 4959–4968. [CrossRef]
34. Seright, R.S.; Eiang, J.; Sun, H.; Socorro, N.M. Gel treatments in production wells with water coning problems. *IN SITU* **1993**, *17*, 243–272.
35. Sydansk, R.D.; Xiong, Y.; Al-Dhafeeri, A.M.; Schrader, R.J.; Seright, R.S. Characterization of partially formed polymer gels for application to fractured production wells for water-shutoff purposes. *SPE Prod. Facil.* **2005**, *20*, 240–249. [CrossRef]
36. Medellín, D.; Ravi, V.R.; Torres-Verdín, C. Multidimensional NMR inversion without Kronecker products: Multilinear inversion. *J. Magn. Reson.* **2016**, *269*, 24–35. [CrossRef] [PubMed]
37. Sheidaie, A.; Fahimpour, J.; Sharifi, M. Experimental Investigation of Low-Concentrated Nanocomposite Polymer Gels for Water Shutoff Treatment Under Reservoir Conditions. *SPE J.* **2022**, *27*, 2390–2407. [CrossRef]
38. Saghandali, F.; Salehi, M.B.; Taghikhani, V. Hydrogel nanocomposite network elasticity parameters as a function of swelling ratio: From micro to macro flooding. *J. Ind. Eng. Chem.* **2023**, *125*, 163–177. [CrossRef]
39. Willhite, G.P.; Zhu, H.; Natarajan, D.; McCool, C.S.; Green, D.W. Mechanisms causing disproportionate permeability reduction in porous media treated with chromium acetate/HPAM gels. *SPE J.* **2002**, *7*, 100–108. [CrossRef]
40. Qin, L.; Myers, M.B.; Otto, C.; Verrall, M.; Zhong, Z.; Arjomand, E.; Saeedi, A.; Wood, C.D. Further insights into the performance of silylated polyacrylamide-based relative permeability modifiers in carbonate reservoirs and influencing factors. *ACS Omega* **2021**, *6*, 13671–13683. [CrossRef] [PubMed]

Disclaimer/Publisher's Note: The statements, opinions and data contained in all publications are solely those of the individual author(s) and contributor(s) and not of MDPI and/or the editor(s). MDPI and/or the editor(s) disclaim responsibility for any injury to people or property resulting from any ideas, methods, instructions or products referred to in the content.